Sheena Mittal and Jasobanta Jena\*

# Interaction of a Singular Surface with a Characteristic Shock in a Relaxing Gas with Dust Particles

https://doi.org/10.1515/zna-2019-0217 Received June 25, 2019; accepted September 22, 2019; previously published online October 10, 2019

Abstract: A system of hyperbolic differential equations outlining one-dimensional planar, cylindrical symmetric and spherical symmetric flow of a relaxing gas with dust particles is considered. Singular surface theory used to study different aspects of wave propagation and its culmination to the steepened form. The evolutionary behavior of the characteristic shock is studied. A particular solution of the governing system of equations is used to discuss the steepened wave form, characteristic shock and their interaction. The results of the interaction between the steepened wave front and the characteristic shock using the general theory of wave interaction are discussed. Also, the influence of relaxation and dust parameters on the steepened wave front, the formation of a characteristic shock, reflected and transmitted waves after interaction and a jump in shock acceleration are investigated.

**Keywords:** Characteristic Shock; Relaxing Dusty Gas; Singular Surface Theory.

#### 1 Introduction

Waves are a natural outcome of technical progression, so are the discontinuities. As the environment is inundated with waves, the study of the interaction of a wave with discontinuities is likely to have a positive impact on the propagation of waves. The topic carries a high empirical utility that makes it an interesting area to explore further. A wave can be viewed as a surface which moves in accordance with some flow variables describing the material medium. Some interrelated discontinuities are also carried

\*Corresponding author: Jasobanta Jena, Department of Mathematics, Netaji Subhas University of Technology, Sector-3, Dwarka, New Delhi–110 078, India, E-mail: jjena67@rediffmail.com

Sheena Mittal: Department of Mathematics, Netaji Subhas
University of Technology, Sector-3, Dwarka, New Delhi–110 078, India, E-mail: sheenamittal90@yahoo.com

along by the surface, which arise out of the flow variables or their derivatives.

Singular surface theory of the first order uses the approach that the functions itself are continuous and undergo jump discontinuity in at least one of its first order derivatives. In a recent paper, this theory was used to study wave propagation and its termination into discontinuities in three different contexts of flow of a non-ideal dusty gas, and further among other results, the effects of the ratio of species densities and the ratio of specific heat on shock formation were shown [1]. The nonlinear theory of wave propagation was discussed by Varley and Cumberbatch [2] and the propagation of weak discontinuities in different materials using singular surface theory has been studied by many authors from an applicative point of view [3–5]. The studies of concern from the precomputer era to date, have been the interaction of these weak discontinuities with shock wave using the general theory of wave interaction. The work done by Jeffrey [6, 7] on the problem of interaction has been further extended by many authors. Radha et al. [8] studied the general theory for problems of wave interactions leading to the results obtained by Boillat and Ruggeri [9]. Boillat and Ruggeri [10] studied the characteristic shock and constructed examples to analyze the same for completely and strictly exceptional systems. For a clear understanding one may refer the fundamental works carried out in [9-13]. Mentrelli et al. [14], taking into consideration a perfect gas, studied the interaction between a shock and an acceleration wave with varying shock strength. Many more results have been concluded using the theory in different material media [15-22]. In dusty gases, self similar solutions and converging shocks followed by wave propagation were discussed in [23-26]. Recently, Shah and Singh studied the collision between a blast wave and a steepened wave in dusty real reacting gases [27], and the interaction of a singular surface with a strong shock in reacting polytropic gases [28].

The relaxation mechanism in gas is basically the rate of process of attaining equilibrium through non-equilibrium which occurs due to some external forces and the time taken to get the equilibrium state back is known as the relaxation time [29–31]. In general, the energy in

a gas molecule is distributed among translational modes. vibrational modes, and rotational modes. The time taken by a particular mode to attain equilibrium is called the relaxation time of that mode. The relaxation times for translational and rotational modes are very short, whereas the same for vibrational modes is much longer [32]. Hence, the propagation of waves in a vibrationally relaxing gas depends on the relaxation time.

In this paper, we discuss the interaction of a singular surface with a characteristic shock in a relaxing gas with dust particles. It is imperative to highlight some of the assumptions being made to formulate the system of the fluid flow [33–36]. It is considered that the solid particles are spherical in nature with uniform size and the specific heat of the gas and the dust particles are constant. We have further assumed that the volume occupied by the solid particles in the mixture is negligible. Using the singular surface approach, the transport equation for the jump in first order derivative of the velocity, which is of a Bernoullitype equation is obtained. The solution of the transport equation is discussed considering a particular case. The evolution of a characteristic shock in the medium is discussed considering the same particular case as in the case of the singular surface. Next, the interaction between the singular surface with the characteristic shock resulting in reflected and transmitted waves and the jump in the shock wave acceleration is studied. The results obtained are analyzed for various dust parameters along with the relaxation effects involved in the flow by performing numerical calculations and depicting the same.

## 2 Basic Equations

The system of partial differential equations representing the one-dimensional, unsteady flow of a dusty relaxing gas with planar (m = 0) and non-planar, i.e. cylindrical symmetry (m = 1) or spherical symmetry (m = 2) with the assumptions made for dust particles in [36, 37] is given by:

$$\rho_t + u\rho_x + \rho u_x + \frac{m\rho u}{x} = 0,$$

$$u_t + uu_x + \frac{1}{\rho}p_x = 0,$$

$$p_t + up_x + \rho a^2 \left(u_x + \frac{mu}{x}\right) = -\frac{(\Gamma - 1)}{(1 - \theta\rho)}\rho Q,$$

$$\sigma_t + u\sigma_x = Q,$$
(1)

along with the equation of the state

$$p = \frac{(1 - k_p)\rho RT}{1 - Z},\tag{2}$$

where t is the time, u is the flow velocity along thexaxis,  $\rho$  and p are the density and pressure of the gas-particle mixture,  $\sigma$  is the vibrational energy,  $Q=\frac{1}{\tau}\Big\{\sigma_e+c\Big(\frac{p(1-Z)}{\rho}-\frac{p_e(1-Z_e)}{\rho_e}\Big)-\sigma\Big\}$ ,  $\Gamma=\frac{\gamma(1+\delta\beta)}{1+\delta\beta\gamma}$ ,  $a=\frac{1}{\tau}\Big\{\sigma_e+c\Big(\frac{p(1-Z)}{\rho_e}-\frac{p_e(1-Z_e)}{\rho_e}\Big)-\sigma\Big\}$  $\left(\frac{\Gamma p}{\rho(1-Z)}\right)^{1/2}$ , R the specific gas constant, T the temperature, and  $Z = V_{sp}/V$  is the volume fraction. If otherwise not stated a variable as a subscript indicates a partial derivative with respect to that variable. However, the variable with 'e' as a subscript denotes the initial value of the variable in the equilibrium state.

Here,  $V_{sp}$  and V are the volumetric extension of the solid particles and total volume of the mixture, respectively; the parameters c and  $\tau$  specifies the ratio of vibrational specific heat to the specific gas constant and the relaxation time,  $k_p = \varphi_{sp}/\varphi$  is the mass fraction of the solid particles in the gas mixture,  $\delta = k_p/(1 - k_p)$ ,  $\beta =$  $c_{sp}/c_p$ ,  $\gamma = c_p/c_v$ ,  $\theta = k_p/\rho_{sp}$  where Z in terms of  $k_p$  can be written as  $Z = \theta \rho$ , entailing  $\varphi_{sp}$  and  $\varphi$  as the total mass of the solid particles and the mixture, respectively,  $c_{sp}$  as the specific heat of solid particles,  $c_p$  the specific heat of the gas at constant pressure, and  $c_v$  the specific heat of the gas at constant volume. Also, we make use of an added variable  $G = \rho_{sp}/\rho_g$ , the ratio of the density of the solid particles to the species density of the gas, to compare the behavior of the flow variables as the time proceeds.

It may be noted that the equations of states for the gas and solid particles are given by  $p_g = \rho_g RT$  and  $\rho_{sp} =$ constant, respectively, where  $p_g$  is the pressure of the gas. As the presence of dust particles have negligible contributions to the pressure of the mixture due to the larger particle size, it is assumed that  $p_g = p$  [34]. The densities of the gas, solid particles and the mixture are related to each other as per the following:

$$ho=rac{(1-Z)
ho_g}{1-k_p}, \quad 
ho=rac{Z}{k_p}
ho_{sp}.$$

If the flow is vibrationless or translationally active, i.e. either in equilibrium ( $\sigma=\overline{\sigma}$ ) presupposing  $\overline{\sigma}=\sigma_e+$  $c\left(\frac{p(1-Z)}{\rho}-\frac{p_e(1-Z_e)}{\rho_e}\right)$  as the equilibrium value of  $\sigma$ , or frozen ( $\sigma = \text{const}$ ) as  $\tau \to \infty$ , no relaxation is involved thereby implying Q = 0.

The system of (1) can also be written in the matrix form as:

$$U_t + AU_x = f, (3)$$

where 
$$U=(\rho,u,p,\sigma)^{tr}$$
,  $f=\left(\frac{-m\rho u}{x},0,-\left(\frac{(\Gamma-1)}{(1-\theta\rho)}\rho Q+\frac{m\rho a^2 u}{x}\right),Q\right)^{tr}$  and

$$A = \begin{pmatrix} u & \rho & 0 & 0 \\ 0 & u & 1/\rho & 0 \\ 0 & \rho a^2 & u & 0 \\ 0 & 0 & 0 & u \end{pmatrix}, \tag{4}$$

in which *tr* represents transposition.

## 3 Transport Equation for the Jump Discontinuity

Let us consider flow variables  $\rho$ , u, p, and  $\sigma$  to be necessarily continuous while allowing discontinuities in their derivatives across the surface associated with a propagating wave and denoted by  $x = \varepsilon(t)$  the equation of the wave front  $\Phi$ . For  $\Phi$  to be a characteristic surface, the moving discontinuities of the first and second order must satisfy the geometrical and kinematical compatibility conditions. The compatibility conditions were derived by Hadamad [38] using the Lagrangian parameters rather than the space coordinates as Eulerian variables. He also considered an extension of the relations using Lagrangian parameters giving the discontinuities in the second and higher derivatives of quantities under the assumption that only the quantities themselves are continuous over  $\Phi$ . The conditions were later presented by Thomas using Eulerian variables [39, 40], which are as follows:

$$|[H_x]| = B, \quad |[H_t]| = -VB, \quad |[H_{xx}]| = \overline{B},$$
  
$$|[H_{xt}]| = V(B_x - \overline{B}), \tag{5}$$

where H takes the value of any of the flow variables, Bis a function defined on the surface  $\Phi$ , provided  $B \neq 0$ implying the existence of discontinuity and  $V = \frac{d\varepsilon}{dt}$  is the speed with which  $\Phi$  propagates. If W is any variable then  $|[W]| = W - W_0$  means the jump in W across the wave front  $\Phi$  and  $W_0$  and W represents the values of W just ahead and just behind  $\Phi$ .

As for an advancing wave *V* is positive, the evaluating system (1) on the inner boundary of  $\Phi$  gives

$$V = a_0 + u_0$$
,  $\alpha^{(1)} = \frac{1}{\rho_0 a_0} \xi = \frac{a_0}{\rho_0} \rho$  and  $\eta = 0$ , (6)

on using the following jump values

$$|[\rho_x]| = \rho, \quad |[u_x]| = \alpha^{(1)}, \quad |[p_x]| = \xi, \quad |[\sigma_x]| = \eta,$$
  
 $|[\rho_t]| = -V\rho, \quad |[u_t]| = -V\alpha^{(1)}, \quad |[p_t]| = -V\xi,$   
 $|[\sigma_t]| = -V\eta.$  (7)

Also.

(4) 
$$|[\rho_{xx}]| = \overline{\rho}, \quad |[u_{xx}]| = \overline{\alpha^{(1)}}, \quad |[p_{xx}]| = \overline{\xi}, \quad |[\sigma_{xx}]| = \overline{\eta},$$
$$|[\rho_{xt}]| = V(\rho_x - \overline{\rho}), \quad |[u_{xt}]| = V(\alpha_x^{(1)} - \overline{\alpha^{(1)}}),$$
$$|[p_{xt}]| = V(\xi_x - \overline{\xi}), \quad |[\sigma_{xt}]| = V(\eta_x - \overline{\eta}). \tag{8}$$

Differentiating system (1) with respect to *x* and evaluating behind the wave front  $\Phi$ , we get:

$$\begin{split} |[\rho_{xt}]| + 2|[u_x\rho_x]| + u_0|[\rho_{xx}]| + \rho_0|[u_{xx}]| \\ + \frac{mu_0}{x}|[\rho_x]| + \frac{m\rho_0}{x}|[u_x]| = 0, \\ |[u_{xt}]| + u_0|[u_{xx}]| + |[u_xu_x]| \\ + \frac{1}{\rho_0}|[p_{xx}]| - \frac{1}{\rho_0^2}|[p_x\rho_x]| = 0, \\ |[p_{xt}]| + \left(1 + \frac{\rho a_0^2}{p_0}\right)|[u_xp_x]| + u_0|[p_{xx}]| \\ + \rho_0 a_0^2 \left(|[u_{xx}]| + \frac{m}{x}|[u_x]|\right) + \frac{\theta \rho_0 a_0^2}{1 - \theta \rho_0}|[u_x\rho_x]| \\ + \frac{mu_0}{x} \left(\frac{\rho_0 a_0^2}{p_0}|[p_x]| + \frac{\theta \rho_0 a_0^2}{1 - \theta \rho_0}|[\rho_x]|\right) \\ = -\frac{(\Gamma - 1)}{(1 - \theta \rho_0)} \{Q_0|[\rho_x]| + \rho_0((Q_\rho)_0|[\rho_x]| \\ + (Q_p)_0|[p_x]| + (Q_\sigma)_0|[\sigma_x]|) + \frac{\rho_0 \theta Q_0|[\rho_x]|}{(1 - \theta \rho_0)} \}, \\ |[\sigma_{xt}]| + |[u_x\sigma_x]| + u_0|[\sigma_{xx}]| \\ = ((Q_\rho)_0|[\rho_x]| + (Q_p)_0|[p_x]| + (Q_\sigma)_0|[\sigma_x]|). \tag{9} \end{split}$$

Use of (8) in (9) yields

$$V(\rho_{x} - \overline{\rho}) + 2((\rho + \rho_{0x})\alpha^{(1)} + \rho u_{0x}) + u_{0}\overline{\rho} + \rho_{0}\overline{\alpha^{(1)}} + \frac{m}{x}(u_{0}\rho + \rho_{0}\alpha^{(1)}) = 0,$$

$$V(\alpha_{x}^{(1)} - \overline{\alpha^{(1)}}) + u_{0}\overline{\alpha^{(1)}} + (\alpha^{(1)})^{2} + \frac{1}{\rho_{0}}\overline{\xi} - \frac{1}{\rho_{0}^{2}}(\rho(\xi + p_{0x}) + \rho_{0x}\xi) + 2\alpha^{(1)}u_{0x} = 0,$$

$$V(\xi_{x} - \overline{\xi}) + \left(1 + \frac{\rho_{0}a_{0}^{2}}{p_{0}}\right)(\alpha^{(1)}(\xi + p_{0x}) + u_{0x}\xi) + u_{0x}\xi) + \frac{\Gamma\theta p_{0}}{(1 - \theta\rho_{0})^{2}}((\alpha^{(1)} + u_{0x} + \frac{mu_{0}}{x})\rho + \rho_{0x}\alpha^{(1)}) + \frac{mu_{0}\rho_{0}a_{0}^{2}\xi}{xp_{0}} = -\frac{(\Gamma - 1)}{(1 - \theta\rho_{0})} + \frac{\rho_{0}\theta Q_{0}\rho}{(1 - \theta\rho_{0})},$$

$$(\rho Q_{0} + \frac{c}{\tau}\left(\frac{-p_{0}\rho}{\rho_{0}} + (1 - \theta\rho_{0})\xi\right) + \frac{\rho_{0}\theta Q_{0}\rho}{(1 - \theta\rho_{0})},$$

$$\alpha^{(1)}\sigma_{0x} - a_{0}\overline{\eta} = \frac{c}{\tau}\left(\frac{-p_{0}\rho}{\rho_{0}} + (1 - \theta\rho_{0})\xi\right). \tag{10}$$

Further, eliminating  $\overline{\rho}$ ,  $\overline{\alpha^{(1)}}$  and  $\overline{\xi}$  from (10) we obtain the following Bernoulli type of transport equation [6] for  $\alpha^{(1)}$ 

$$2\frac{\mathrm{d}\alpha^{(1)}}{\mathrm{d}t} + \left(\frac{\Gamma+1}{1-\theta\rho_0}\right)(\alpha^{(1)})^2 + \Theta\alpha^{(1)} = 0,$$
 (11)

where

$$\begin{split} \Theta &= u_{0x} \left( 3 + \frac{\Gamma}{1 - \theta \rho_0} + \frac{\Gamma \theta p_0}{(1 - \theta \rho_0)^2 a_0^2} \right) \\ &+ \frac{m}{x} \left( \frac{u_0 \Gamma}{1 - \theta \rho_0} + a_0 + \frac{u_0 \Gamma \theta p_0}{a_0^2 (1 - \theta \rho_0)^2} \right) \\ &+ \rho_{0x} \left( \frac{\Gamma \theta p_0}{\rho_0 a_0 (1 - \theta \rho_0)^2} - \frac{a_0}{\rho_0} \right) + \frac{\Gamma p_{0x}}{(1 - \theta \rho_0) \rho_0 a_0} \\ &+ \frac{(\Gamma - 1)}{(1 - \theta \rho_0)} \left( \frac{Q_0}{a_0^2 (1 - \theta \rho_0)} + \frac{(\Gamma - 1)(1 - \theta \rho_0)c}{\tau \Gamma} \right). \end{split}$$

#### 3.1 A Particular Case

Using the following form of flow variables just ahead of the wave front  $\boldsymbol{\Phi}$ 

$$u_0(x, t) = \ell(t)x, \quad \rho_0 = \rho_0(t), \quad p_0 = p_0(t), \quad \sigma_0 = \sigma_0(t),$$

we integrate the governing system of (1) and hence obtain

$$\rho_0(t) = \rho_{0e} (1 + (t - t_{0e})\ell_{0e})^{-(m+1)},$$
  

$$\ell(t) = \ell_{0e} (1 + (t - t_{0e})\ell_{0e})^{-1},$$
(13)

and

$$\begin{split} \frac{\mathrm{d}p_0}{\mathrm{d}t} + \left(\frac{(m+1)\Gamma\ell}{1-\theta\rho_0} + \frac{(\Gamma-1)c}{\tau}\right)p_0 \\ - \frac{(\Gamma-1)\rho_0}{\tau(1-\theta\rho_0)} \left((\sigma_0 - \sigma_e) + \frac{cp_e(1-\theta\rho_e)}{\rho_e}\right) &= 0, \\ \frac{\mathrm{d}\sigma_0}{\mathrm{d}t} + \frac{(\sigma_0 - \sigma_e)}{\tau} \\ - \frac{c}{\tau} \left(\frac{p_0(1-\theta\rho_0)}{\rho_0} - \frac{p_e(1-\theta\rho_e)}{\rho_e}\right) &= 0, \end{split} \tag{14}$$

where  $\rho_{0e}$  and  $\ell_{0e}$  are the reference values of density and velocity at  $t=t_{0e}$ . Using the variables in the dimensionless form

$$x^{\star} = \frac{x}{t_{0e}a_{0e}}, \quad t^{\star} = \frac{t}{t_{0e}}, \quad \ell^{\star} = \ell t_{0e}, \quad \rho_{0}^{\star} = \frac{\rho_{0}}{\rho_{0e}}, \\ p_{0}^{\star} = \frac{p_{0}}{\rho_{0e}a_{0e}^{2}}, \quad \sigma_{0}^{\star} = \frac{\sigma_{0}}{a_{0e}^{2}}, \quad a_{0}^{\star} = \frac{a_{0}}{a_{0e}}, \\ \theta^{\star} = \rho_{0e}\theta, \quad (\alpha^{(1)})^{\star} = t_{0e}\alpha^{(1)}, \quad \tau^{\star} = \frac{\tau}{t_{0e}}, \\ \rho_{e}^{\star} = \frac{\rho_{e}}{\rho_{0e}}, \quad p_{e}^{\star} = \frac{p_{e}}{\rho_{0e}a_{0e}^{2}}, \quad \sigma_{e}^{\star} = \frac{\sigma_{e}}{a_{0e}^{2}},$$

and then suppressing the asterisk sign, the transport (11) reduces to

$$2\frac{\mathrm{d}lpha^{(1)}}{\mathrm{d}t} + \left(\frac{\Gamma+1}{1- heta
ho_0}\right)(lpha^{(1)})^2 + \Omegalpha^{(1)} = 0,$$
 (15)

where

$$\begin{split} \Omega &= \ell \Bigg( 3 + \frac{\Gamma}{1 - \theta \rho_0} + \frac{\Gamma \theta p_0}{\left( 1 - \theta \rho_0 \right)^2 a_0^2} + \frac{m \Gamma}{1 - \theta \rho_0} \Bigg) \\ &+ \frac{m a_0}{x} + \frac{m \ell \Gamma \theta p_0}{\left( 1 - \theta \rho_0 \right)^2 a_0^2} + \frac{(\Gamma - 1)}{(1 - \theta \rho_0)} \\ & \left( \frac{Q_0}{a_0^2 (1 - \theta \rho_0)} + \frac{(\Gamma - 1)(1 - \theta \rho_0)c}{\tau \Gamma} \right). \end{split}$$

The value of x appearing in the coefficient  $\Omega$  in (15) is computed using the relation  $\frac{dx}{dt} = u_0 + a_0$  from (6). Integrating (15), we obtain the following solution

$$\alpha^{(1)}(t) = \alpha_0^{(1)} \exp\left(-\frac{1}{2} \int_{t_0}^t \Omega(w) dw\right)$$

$$\left\{1 + \alpha_0^{(1)} \int_{t_0}^t \left(\frac{\Gamma + 1}{2(1 - \theta \rho_0)}\right) \eta(w) dw\right\}^{-1}, \quad (16)$$

with  $\eta(t) = \exp\left(-\frac{1}{2}\int_{t_0}^t \Omega(w)dw\right)$ .

Also, numerical integration of (15) using (13) and (14) is performed for  $1 \le t \le \infty$  and the results showing the behavior of jump in the velocity gradient are analyzed by plotting  $\alpha^{(1)}$  against 1/t. The analysis yields the following conclusions:

In the case of rarefaction wave, i.e  $\alpha_0^{(1)} > 0$ , (16) signifies that  $\eta(t) \to 0$  along with  $I(t) = \int_{t_0}^t \left(\frac{\Gamma+1}{2(1-\theta\rho_0)}\right) \eta(w) dw < \infty$  resulting in  $\alpha^{(1)}(t) \to 0$ as t approaches infinity for all the possible range of values of parameters involved in the flow such as  $k_p$ ,  $\beta$ , G, c, and  $\tau$  and hence concluding that with an increase in the time the wave flattens and eventually dies out. The behavior is shown graphically in Figures 1–4 for variations with the parameters  $k_p$ ,  $\beta$ , G, and  $\tau$ . It is observed that an increase in any of the parameters  $k_p$ ,  $\beta$ , or G leads to an increase in  $\alpha^{(1)}/\alpha_0^{(1)}$ . As from the expression for *Q* in (1), an increase in the relaxation parameter c is equivalent to a decrease in the parameter  $\tau$ , we have not added any figures showing variations with c. The presence of dust particles in the system drives the velocity gradient to increase thereby taking more time to converge to zero. However, an opposite trend is noticed with an increase in the parameter  $\tau$ .

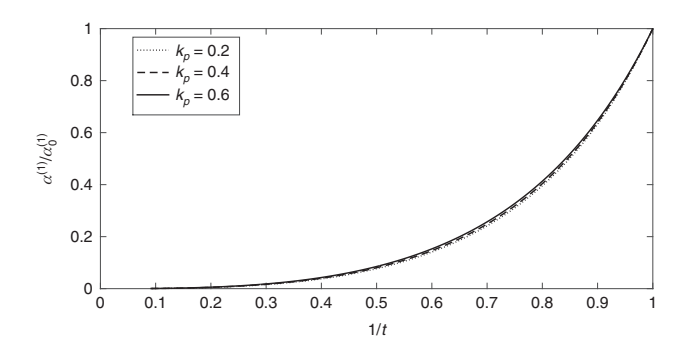


**Figure 1:** Variation of  $\alpha^{(1)}/\alpha_0^{(1)}$  with 1/t influenced by the parameter  $k_p$  where  $m=1, c=0.01, G=1000, \beta=0.5, \tau=10$ .

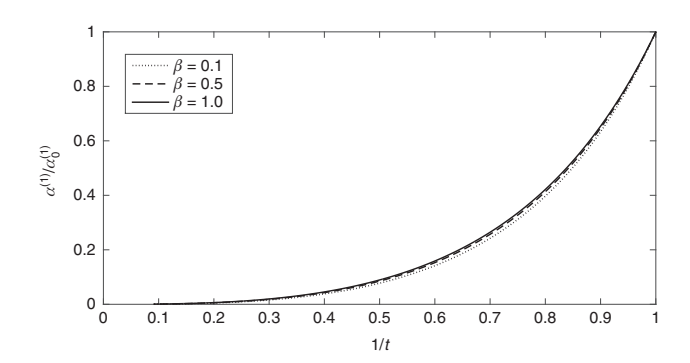


**Figure 2:** Variation of  $\alpha^{(1)}/\alpha_0^{(1)}$  with 1/t influenced by the parameter  $\beta$  where m=1, c=0.01, G=1000,  $k_p=0.6$ ,  $\tau=10$ .

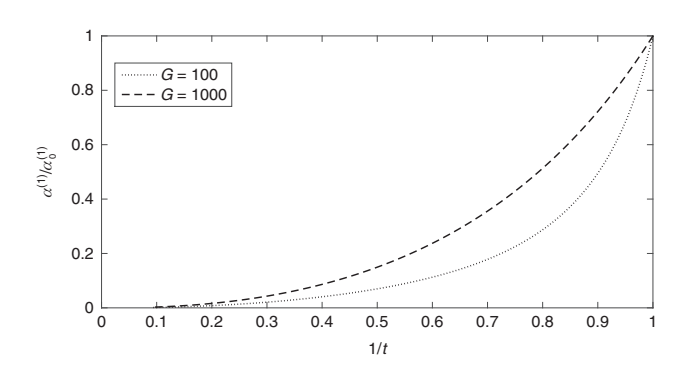


**Figure 3:** Variation of  $\alpha^{(1)}/\alpha_0^{(1)}$  with 1/t influenced by the parameter *G* where  $m=1, c=0.01, k_p=0.6, \beta=0.5, \tau=10$ .

(ii) For a compression wave ( $\alpha_0^{(1)} < 0$ ) the solution given by (16) breaks down when  $1 + \alpha_0^{(1)}I(t)$  equals zero at some time  $t = t_c$ , implying the existence of steepened wave in a finite time only.

We study in detail the following cases arising from (16):

- 1. The condition ' $|\alpha_0^{(1)}|/\alpha_c^{(1)}<1$ ', where  $\alpha_c^{(1)}=1/I\{\infty\}$  leads to  $\alpha^{(1)}\to 0$  pointing towards the existence of flattened wave as time advances.
- 2. For ' $|\alpha_0^{(1)}|/\alpha_c^{(1)}>1$ ',  $\exists$  a finite time  $t_c$  such that  $I(t_c)=1/|\alpha_0^{(1)}|$  and  $|\alpha^{(1)}|\to\infty$  as  $t\to t_c$ . This

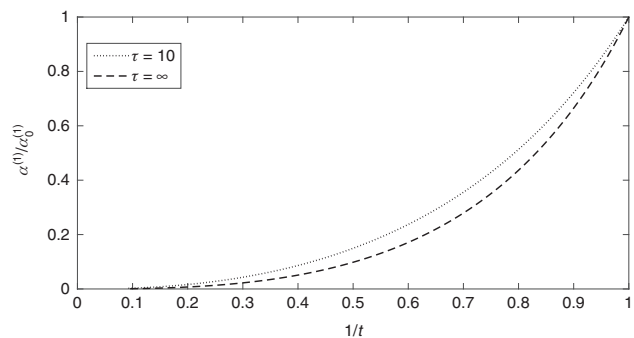


**Figure 4:** Variation of  $\alpha^{(1)}/\alpha_0^{(1)}$  with 1/t influenced by the parameter  $\tau$  where  $m=1, G=1000, \beta=0.5, c=0.01, k_p=0.6$ .

yields the existence of a shock wave in a finite time only at an instant  $t_c$ .

3. For ' $|\alpha_0^{(1)}|/\alpha_c^{(1)}=1$ ', the wave behaves in the same way as in (1).

These discussed outcomes for compression waves are illustrated in Figures 5–12. It is again observed that an increase in any of the parameters  $k_p$ ,  $\beta$  or G leads an increase in  $\alpha^{(1)}/\alpha_0^{(1)}$  for the interval  $-\alpha_c^{(1)} \leqslant \alpha_0^{(1)} < 0$ , and a decrease in

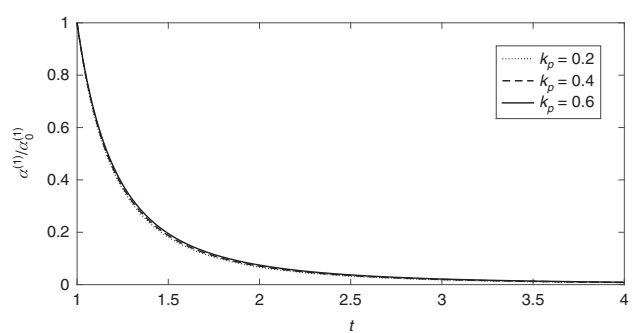


**Figure 5:** Variation of  $\alpha^{(1)}/\alpha_0^{(1)}$  with t influenced by the parameter  $k_p$  in the case of  $\alpha_0^{(1)}>0$  where m=1,  $\tau=10$ , c=0.01,  $\beta=0.5$ , G=1000.

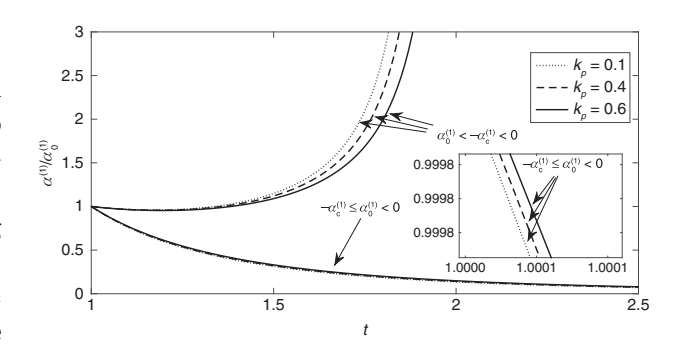


**Figure 6:** Variation of  $\alpha^{(1)}/\alpha_0^{(1)}$  with t influenced by the parameter  $k_p$  in the case of  $\alpha_0^{(1)}<0$  where  $m=1,\,\tau=10,\,c=0.01,\,\beta=0.5,\,G=1000.$ 

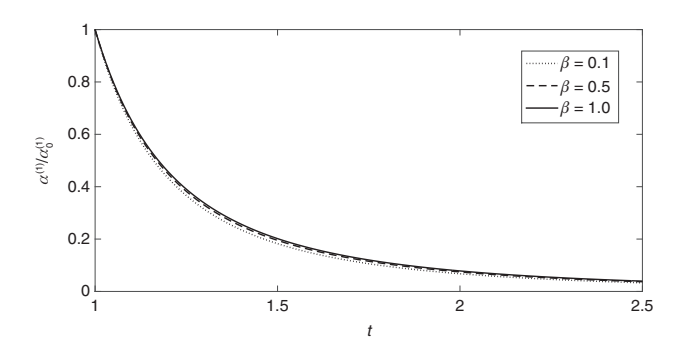


**Figure 7:** Variation of  $\alpha^{(1)}/\alpha_0^{(1)}$  with t influenced by the parameter  $\beta$ , in the case of  $\alpha_0^{(1)}>0$  where  $m=1, c=0.01, k_p=0.6, \tau=10, G=1000.$ 

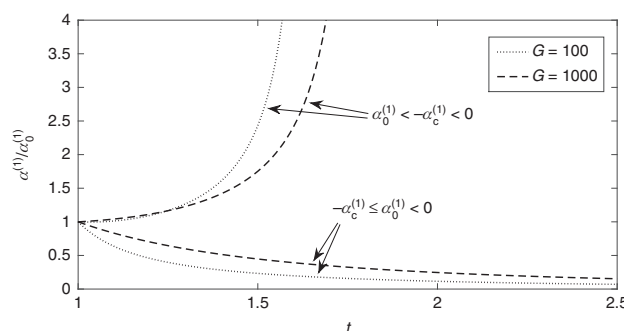


**Figure 10:** Variation of  $\alpha^{(1)}/\alpha_0^{(1)}$  with t influenced by the parameter G in the case of  $\alpha_0^{(1)}<0$  where m=1,  $k_p=0.6$ , c=0.01,  $\beta=0.5$ ,  $\tau=10$ .

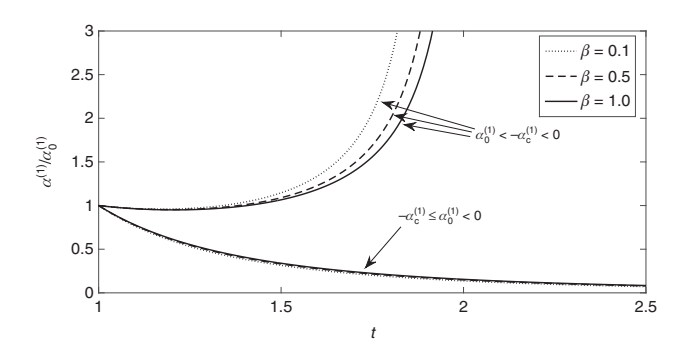


**Figure 8:** Variation of  $\alpha^{(1)}/\alpha_0^{(1)}$  with t influenced by the parameter  $\beta$  in the case of  $\alpha_0^{(1)}<0$  where m=1, c=0.01,  $k_p=0.6$ ,  $\tau=10$ , G=1000.

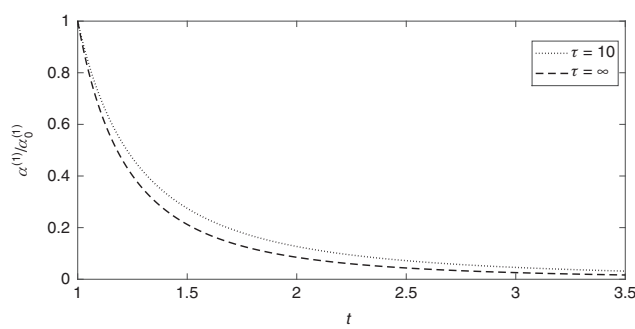


**Figure 11:** Variation of  $\alpha^{(1)}/\alpha_0^{(1)}$  with t influenced by the parameter  $\tau$ , in the case of  $\alpha_0^{(1)}>0$  when  $m=1, c=0.01, k_p=0.6, \beta=0.5, G=1000.$ 

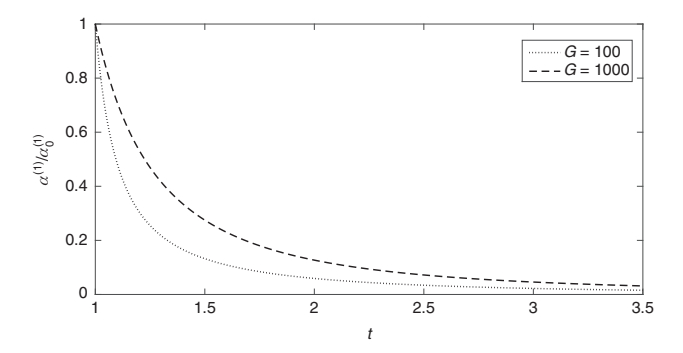


**Figure 9:** Variation of  $\alpha^{(1)}/\alpha_0^{(1)}$  with t influenced by the parameter G in the case of  $\alpha_0^{(1)}>0$  where  $m=1, k_p=0.6, c=0.01, \beta=0.5, \tau=10.$ 

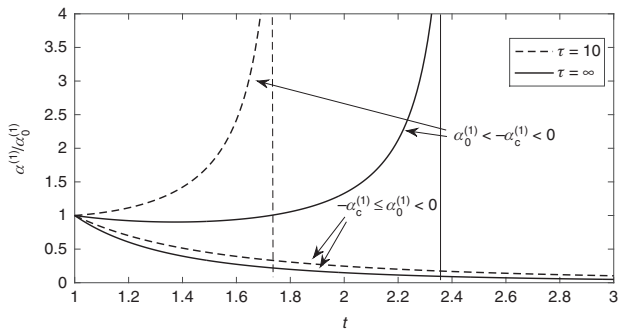


**Figure 12:** Variation of  $\alpha_0^{(1)}/\alpha_0^{(1)}$  with t influenced by the parameter  $\tau$ , in the case of  $\alpha_0^{(1)}<0$  when  $m=1, c=0.01, k_p=0.6, \beta=0.5, G=1000.$ 

 $\alpha^{(1)}/\alpha_0^{(1)}$  for the interval  $\alpha_0^{(1)} \leqslant -\alpha_c^{(1)} < 0$ ; however, an increase in the variable  $\tau$  leads to an opposite trend.

(iii) Also the behavior of  $\alpha^{(1)}/\alpha_0^{(1)}$  is observed to be decreasing and approaching to zero as time increases eventually to infinity.

## **4 Characteristic Shock**

Characteristic shock arises when the characteristic surface and the shock surface both occur simultaneously and the shock surface velocity, both behind and ahead of the shock, coincides with a latent root of the system [11, 41].

Characteristic shock exists when the corresponding eigenvalue is linearly degenerate (also referred to as exceptional). Mathematically it states:

$$\nabla \lambda^{(i)}.R^{(i,j)}=0.$$

where  $\nabla$  represents the gradient operator,  $R^{(i,j)}$  the right eigenvectors with respect to the eigenvalue  $\lambda^{(i)}$  having multiplicity  $m_i$  with  $i = 1, ..., m_i$ . In particular, for the conservative hyperbolic system of equations, a wave with eigenvalue having multiplicity m > 1 is always exceptional (linearly degenerate) [9, 13]. The eigenvalues of the matrix A in (4) are:

$$\lambda^{(1)}=(u+a), \quad \lambda^{(2)}=u \text{ (adouble root)} \quad \text{and}$$

$$\lambda^{(3)}=(u-a). \tag{17}$$

As the multiplicity of  $\lambda^{(2)} = u$  is 2, this implies the existence of characteristic shock with speed  $\theta = u$ . Further, the eigenvectors of A are given by:

$$L^{(1)} = (0, \rho a, 1, 0), R^{(1)} = (1/(2a^2), 1/(2\rho a), 1/2, 0)^{tr},$$

$$L^{(2,1)} = (-a^2, 0, 1, 0), R^{(2,1)} = (-a^{-2}, 0, 0, 0)^{tr},$$

$$L^{(2,2)} = (0, 0, 0, 1), R^{(2,2)} = (0, 0, 0, 1)^{tr},$$

$$L^{(3)} = (0, -\rho a, 1, 0),$$

$$R^{(3)} = (1/(2a^2), -1/(2\rho a), 1/2, 0)^{tr}.$$
(18)

Considering *X* as the value just behind the characteristic shock and  $X_*$  ahead of the characteristic shock, let  $[X] = X - X_*$  is the jump in X along the characteristic shock. Here, the Rankine-Hugoniot jump conditions are [u] = 0, [p] = 0,  $[\rho] = \zeta$ , and  $[\sigma] = \omega$  where  $\zeta$  and  $\omega$  are unknown functions of *t* to be determined.

On forming the jump across the characteristic shock in usual manner one obtains:

$$L\frac{\mathrm{d}[U]}{\mathrm{d}t} + [L]\frac{\mathrm{d}U^{\star}}{\mathrm{d}t} = L[f] + [L]f_{\star},\tag{19}$$

where  $d/dt = \partial/\partial t + u\partial/\partial x$  is the material derivative operator.

Using (19), the transport equations for  $\zeta$  and  $\omega$  are obtained as follows

$$\begin{split} \frac{\mathrm{d}\zeta}{\mathrm{d}t} &= -\frac{mu}{x_0} \left( \frac{\zeta(1+\theta\zeta)}{1-\theta(\rho-\zeta)} \right) + u_x \left( \frac{\zeta(2\theta\rho-\theta\zeta-1)}{1-\theta(\rho-\zeta)} \right) \\ &+ \frac{(\Gamma-1)\rho}{\tau\Gamma p(1-\theta\rho+\theta\zeta)} \{ \zeta(\sigma_e - cp_e(1-\theta\rho_e)/\rho_e - \sigma \\ &+ \omega(1-\theta\rho)) - \rho\omega(1-\theta\rho) \}, \end{split}$$

$$\frac{\mathrm{d}\omega}{\mathrm{d}t} = -\frac{1}{\tau} \left\{ \omega + \frac{cp\zeta}{\rho(\rho - \zeta)} \right\}. \tag{20}$$

Using (12) in (20) and applying the following dimensionless variables in the resulting equation:

$$\hat{\zeta}=\zeta/
ho_0,\quad \hat{p}=p/p_0,\quad \hat{\omega}=\omega
ho_0/p_0,$$
  $\hat{\sigma}=\sigma
ho_0/p_0,\quad \hat{
ho}=\rho/
ho_0,$   $\hat{t}=t/t_0,\quad \hat{ au}=\tau/t_0,\quad \hat{\ell}=\ell t_0,$   $\hat{\sigma}_0=\sigma_0
ho_0/p_0,\quad \hat{\sigma}_e=\sigma_e
ho_0/p_0,$ 

and then suppressing the hat sign, we obtain the following equations

$$\frac{\mathrm{d}\zeta}{\mathrm{d}t} = -\left(\frac{\zeta\ell}{1 - \theta(\rho - \zeta)}\right) (1 + \theta\zeta - 2\rho\theta + m(1 + \theta\zeta)) 
+ \frac{(\Gamma - 1)\rho}{\tau\Gamma\rho(1 - \theta(\rho - \zeta))} (\zeta(\sigma_e - cp_e(1 - \theta\rho_e)/\rho_e - \sigma 
+ \omega(1 - \theta\rho)) - \rho\omega(1 - \theta\rho)),$$

$$\frac{\mathrm{d}\omega}{\mathrm{d}t} = -\frac{1}{\tau} \left\{\omega + \frac{cp\zeta}{\rho(\rho - \zeta)}\right\}.$$
(21)

The simultaneous differential (21) are solved using (13) and (14) together with the initial conditions at time t = 1 to study the evolutionary behavior of a characteristic shock. The results are depicted in Figures 13-20 for cylindrical (m = 1) flows. The profiles for other geometries, i.e. planar (m = 0) and spherical (m = 2) flows are found to be similar to the cylindrical case and hence are not plotted. The calculations are performed by taking  $\gamma = 1.4$ ,  $\sigma_0 = 0.005$ ,  $\zeta_0=0.01,~\omega_0=0.01.$  The value of  $\zeta$  and  $\omega$  across the characteristic shock line tends to zero as time proceeds. As observed from Figures 13-16, with rise in the values of  $k_{\nu}$ ,  $\beta$ , or  $\tau$  leads to a rise in  $\zeta$ , whereas a rise in G leads to a fall in  $\zeta$ . From the Figures 17–20, it is observed that a rise in the values of  $k_p$ ,  $\beta$ , or G, gives a fall to the parameter  $\omega$ and a rise in  $\tau$  gives a rise to  $\omega$ .

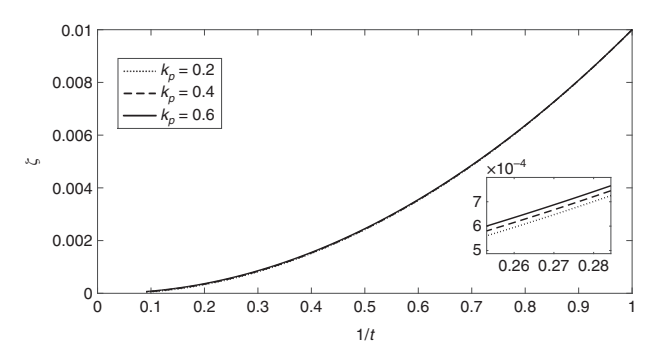


**Figure 13:** Variation of  $\zeta$  vs. 1/t influenced by the parameter  $k_p$ where m = 1, c = 0.01,  $\beta = 0.5$ ,  $\tau = 10$ , G = 1000.

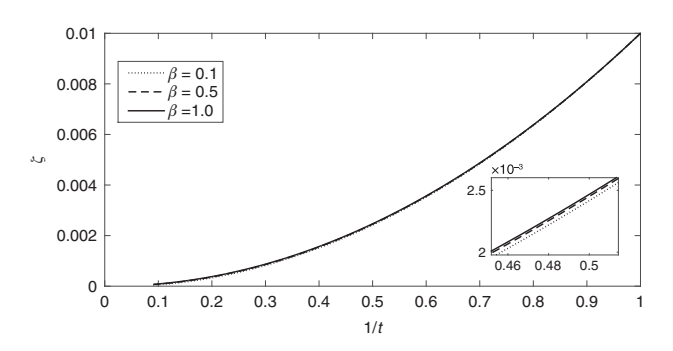


**Figure 14:** Variation of  $\zeta$  vs. 1/t influenced by the parameter  $\beta$  where m=1, G=1000, c=0.01,  $k_p=0.6$ ,  $\tau=10$ .

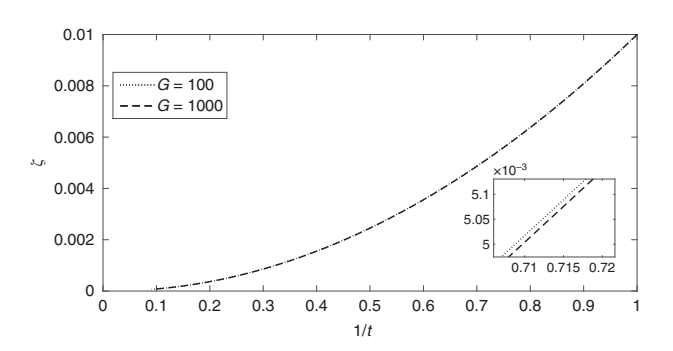


**Figure 15:** Variation of  $\zeta$  with 1/t influenced by the parameter G where m=1,  $\beta=0.5$ , c=0.01,  $k_p=0.6$ ,  $\tau=10$ .

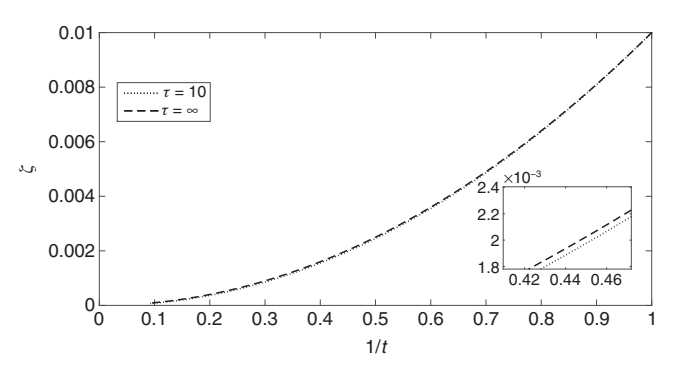


**Figure 16:** Variation of  $\zeta$  with 1/t influenced by the parameter  $\tau$  where m=1, c=0.01, G=1000,  $k_p=0.6$ ,  $\beta=0.5$ .

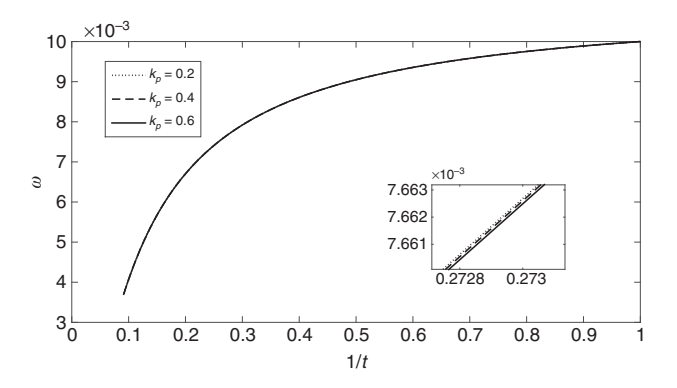


**Figure 17:** Variation of  $\omega$  vs. 1/t influenced by the parameter  $k_p$  where m=1, G=1000, c=0.01,  $\beta=0.5$ ,  $\tau=10$ .

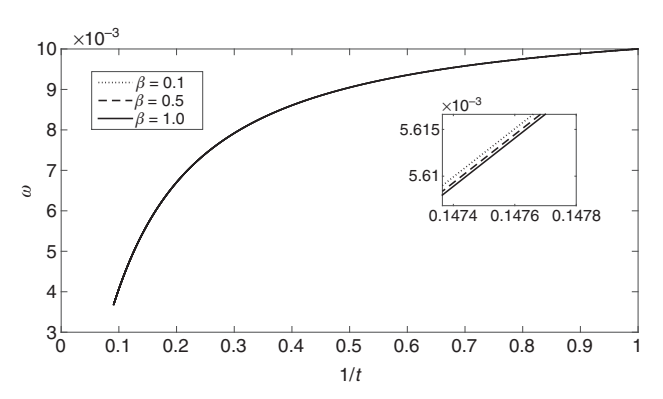


**Figure 18:** Variation of  $\omega$  vs. 1/t influenced by the parameter  $\beta$  where m=1,  $k_p=0.6$ , c=0.01,  $\tau=10$ , G=1000.

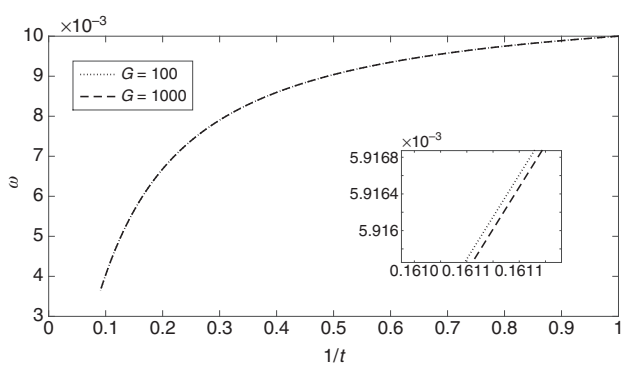


**Figure 19:** Variation of  $\omega$  vs. 1/t influenced by the parameter G where  $\tau=10, m=1, c=0.01, k_p=0.6, \beta=0.5.$ 

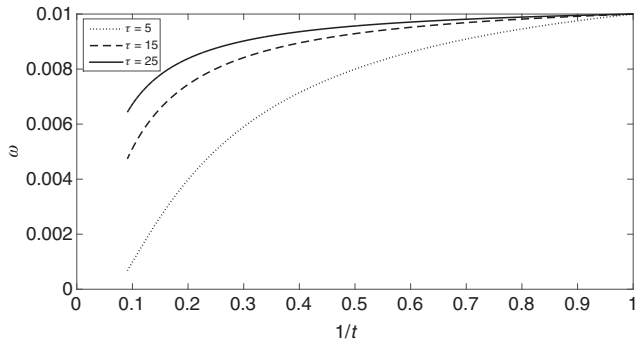


**Figure 20:** Variation of  $\omega$  vs. 1/t influenced by the parameter  $\tau$  where  $k_p=0.6$ ,  $\beta=0.5$ , G=1000, c=0.01, m=1.

# 5 Interaction Between Singular Surface and Characteristics Shock

With disturbances prevailing in every system, it is very obvious to study the impact of those disturbances or shock on the waves traveling in different material media when they interact with each other. In order to investigate the

effect of the interaction between the singular surface traveling along the fastest characteristic with the characteristics shock, we adopted the method discussed in [16] for the interaction between shock waves and weak discontinuities. We consider the system of (1) in the following generalized conservation form behind and ahead of the shock:

$$G_t(x, t, U) + F_x(x, t, U) = K(x, t, U),$$

$$G_{\star t}(x,t,U_{\star}) + F_{\star \chi}(x,t,U_{\star}) = K_{\star}(x,t,U_{\star}), \qquad (22)$$

where U and  $U_*$  represent the solution vectors behind and ahead of the characteristic shock, respectively, and G, F and K are given by the following column vectors

$$\begin{split} G &= \left(\rho, \rho u, \rho \left(\frac{p(1-\theta \rho)}{\rho(\Gamma-1)} + \frac{u^2}{2}\right), \rho \sigma\right)^{tr}, \\ F &= \left(\rho u, \rho u^2 + p, \rho u \left(\frac{p(1-\theta \rho)}{\rho(\Gamma-1)} + \frac{u^2}{2} + \frac{p}{\rho}\right), \rho u \sigma\right)^{tr}, \\ K &= \left(\frac{-m\rho u}{x}, \frac{-m\rho u^2}{x}, -\rho \left(Q + \frac{mu}{x} \left(\frac{p(1-\theta \rho)}{\rho(\Gamma-1)} + \frac{u^2}{2} + \frac{p}{\rho}\right)\right), \\ \rho \left(Q - \frac{mu\sigma}{x}\right)\right)^{tr}. \end{split}$$

Let us consider the two adjacent intervals  $I_u$  and  $I_{u*}$ in accordance with the initial line, i.e. the characteristic shock:

$$I_u = \{x | d_1 < x < x_1 : t = t_0\};$$

$$I_{u^*} = \{x | x_1 < x < d_2; t = t_0\},$$
(23)

where  $d_1$  and  $d_2$  are the constants chosen assuring the propagation of the wave surface in the defined domain of determinacy R. The solution vectors U and  $U_*$  are continuous in the region behind and ahead of the characteristic shock denoted by  $R_u$  and  $R_{u^*}$ , respectively, with the initial conditions  $U(x, t_0) = \phi(x)$  and  $U_*(x, t_0) = \phi_*(x)$ , but, on the other hand, discontinuous across the characteristic shock or the initial line that divides R. Let  $M(x_m, t_m)$  be the point where the fastest wave, i.e. the singular surface originating from  $(x_0, t_0)$  and moving along the characteristic  $\frac{dx}{dt} = \lambda^{(1)}$  denoted as  $\phi(x, t) = 0$  interacts with the characteristic shock propagating with speed  $\theta = u$ . After the interaction, the new wavefront from the point *M* moves along the characteristic  $\frac{dx}{dt} = \lambda_{\star}^{(1)}$  and is represented as  $\phi_*(x,t) = 0$ . The jumps in  $U_x$  across

the incident, reflected and transmitted waves at M, are given by:

$$\wedge_{1}(M) = \sum_{k=1}^{n_{1}} \alpha_{k}^{(1)}(t_{m}) R_{s}^{(1,k)}, \quad \wedge_{i}^{(R)}(M) = \sum_{k=1}^{n_{i}} \alpha_{k}^{(i)}(t_{m}) R_{s}^{(i,k)},$$

$$\wedge_{i}^{\star(T)}(M) = \sum_{k=1}^{n_{i}^{\star}} \beta_{k}^{(i)}(t_{m}) R_{s}^{\star(i,k)}, \qquad (24)$$

with subscript s denoting the values calculated at the point M. The evolutionary equations determining the jump in the shock acceleration  $|[\dot{V}]|$  and the amplitudes  $\alpha_k^{(i)}$  and  $\beta_{k}^{(i)}$  of reflected and transmitted waves are given by the following system of algebraic equations [9]:

$$|[\dot{V}]|(G - G_{\star})_{s} + (\nabla G)_{s} \sum_{i=p-q+1}^{p} \left( \sum_{k=1}^{m_{i}} \alpha_{k}^{(i)} (V - \lambda(i))^{2} R_{s}^{(i,k)} \right)$$

$$- (\nabla^{\star} G^{\star})_{s} \sum_{j=1}^{q} \left( \sum_{k=1}^{m_{j}} \beta_{k}^{(j)} (V - \lambda_{\star}^{(j)})^{2} R_{s}^{\star(j,k)} \right)$$

$$= -(\nabla G)_{s} \sum_{k=1}^{m_{i}} \alpha_{k}^{(i)} (V - \lambda(i))^{2} R_{s}^{(i,k)}. \tag{25}$$

Lax's [42] evolutionary conditions formulated as

$$\begin{split} & \lambda^{(p)} < \lambda^{(p-1)} < \ldots < \lambda^{(l+1)} < V < \lambda^{(l)} < \ldots < \lambda^{(1)}, \\ & \lambda^{(p)}_{\star} < \lambda^{(p-1)}_{\star} < \ldots < \lambda^{(l)}_{\star} < V < \lambda^{(l-1)}_{\star} < \ldots < \lambda^{(1)}_{\star}, \end{split} \tag{26}$$

are satisfied for the index *l*, where  $1 \le l \le p$ , i.e.

$$\lambda^{(3)} < \lambda^{(2)} < V < \lambda^{(1)}, \quad \text{and} \quad \lambda_{\star}^{(3)} < \lambda_{\star}^{(2)} < \lambda_{\star}^{(1)} < V.$$
 (27)

This implies that when the incident wave (singular surface) moving with velocity  $\lambda^{(1)}$  at time  $t = t_m$  collides with the characteristic shock, a reflected wave and a transmitted wave are generated moving with velocity  $\lambda^{(3)}$  and  $\lambda_{\star}^{(1)}$ , respectively. The jump in the shock acceleration  $|[\dot{V}]|$ and the amplitudes of reflected and transmitted wave, i.e.  $\alpha^{(3)}$  and  $\beta^{(1)}$  at time  $t=t_m$  can be evaluated from the following set of equations:

$$(G - G_{\star})_{s}|[\dot{V}]| + (\nabla G)_{s}R_{s}^{(3)}(V - \lambda_{s}^{(3)})^{2}\alpha^{(3)}$$

$$- (\nabla^{\star}G_{\star})_{s}R_{s}^{\star(1)}(V - \lambda_{\star s}^{(1)})^{2}\beta^{(1)}$$

$$= -(\nabla G)_{s}R_{s}^{(1)}(V - \lambda_{s}^{(1)})^{2}\alpha^{(1)}.$$
(28)

Substituting the values from (17), (18) and (22), we obtain the following system of algebraic equations

$$\begin{aligned} & 2\zeta|[\dot{V}]| + \alpha^{(3)} - \beta^{(1)} = -\alpha^{(1)}, \\ & 2u\zeta|[\dot{V}]| + (u - a)\alpha^{(3)} - (u + a*)\beta^{(1)} = -(u + a)\alpha^{(1)}, \\ & 2\left(\frac{\zeta u^{2}}{2} - \frac{p\theta\zeta}{(\Gamma - 1)}\right)|[\dot{V}]| + \left(\left(\frac{u^{2}}{2} - \frac{p\theta}{(\Gamma - 1)}\right) - ua + \left(\frac{(1 - \theta\rho)}{(\Gamma - 1)}\right)a^{2}\right)\alpha^{(3)} \\ & - \left(\left(\frac{u^{2}}{2} - \frac{p\theta}{(\Gamma - 1)}\right) + ua* + \left(\frac{1 - \theta(\rho - \zeta)}{(\Gamma - 1)}\right)a^{2}\right)\beta^{(1)} \\ & = -\left(\left(\frac{u^{2}}{2} - \frac{p\theta}{(\Gamma - 1)}\right) + ua + \left(\frac{(1 - \theta\rho)}{(\Gamma - 1)}\right)a^{2}\right)\alpha^{(1)}, \\ & 2(\zeta\sigma* + \omega\rho* + \zeta\omega)|[\dot{V}]| + \sigma\alpha^{(3)} - \sigma*\beta^{(1)} = -\sigma\alpha^{(1)}. \end{aligned}$$
(29)

It may be noted that the above system equations is an over determined system, which occurs in the case of a characteristic shock. Solving the system of (29), we obtain the values to be:

$$\beta^{(1)} = \frac{2(1 - \theta\rho)a^{2}}{a \cdot \{(1 - \theta\rho)a + (1 - \theta\rho + \theta\zeta)a \cdot \}} \alpha^{(1)},$$

$$|[\dot{V}]| = \left(\frac{(1 - \theta\rho)a^{2} - (1 - \theta\rho + \theta\zeta)a^{2}}{\zeta a \cdot \{(1 - \theta\rho)a + (1 - \theta\rho + \theta\zeta)a \cdot \}}\right) \alpha^{(1)},$$

$$\alpha^{(3)} = \left(\frac{(1 - \theta\rho + \theta\zeta)a \cdot - (1 - \theta\rho)a}{(1 - \theta\rho + \theta\zeta)a \cdot + (1 - \theta\rho)a}\right) \alpha^{(1)}.$$
(30)

As observed from (31), the amplitude of reflected wave  $\beta^{(1)}$ , amplitude of the transmitted wave  $\alpha^{(3)}$ , and jump in the shock acceleration  $|[\dot{V}]|$  are directly proportional to the amplitude of the incident wave  $\alpha^{(1)}$ , thereby implying that any increase or decrease in  $\alpha^{(1)}$  will lead to an increase or decrease in  $\beta^{(1)}$ ,  $\alpha^{(3)}$ , and  $|[\dot{V}]|$ . Also as expected, in the absence of the incident wave, there is neither a jump in

the shock acceleration nor do reflected and transmitted waves exist. As it is evident from (31), the parameters  $\beta^{(1)}$ ,  $\alpha^{(3)}$ , and  $|[\dot{V}]|$  also vary with the dust parameters separately from  $\alpha^{(1)}$ . The variations of the parameters with  $k_p$ ,  $\beta$ , and G are shown in Table 1: (a), (b), and (c), respectively. It is observed that depending on the incident wave being expansive (compressive), the reflected and transmitted waves are compressive (expansive), and the shock decelerates (accelerates) after the impact. The parameters  $\beta^{(1)}$ ,  $\alpha^{(3)}$ , and  $|[\dot{V}]|$  increase with an increase in  $k_p$ , and  $\beta$  in the case of  $\alpha_0^{(1)} > 0$  and decrease in the case of  $\alpha_0^{(1)} < 0$ ; however, an opposite trend is noticed in the case of an increase in G.

### 6 Results and Conclusion

The interaction between a propagating  $\mathcal{C}^{(1)}$  discontinuity and an established shock across the discontinuity line give rise to reflected and transmitted waves as well as producing the jump in shock wave acceleration. In this paper, we considered the system of partial differential equations classifying the one-dimensional, inviscid, unsteady flow of a relaxing gas with dust particles and with varied wavefront curvature. The main aim of this work was to study the effects of dust and relaxation parameters on the incident discontinuity (i.e. the singular surface), characteristic shock and their interaction in the medium.

We considered the evolution and propagation of the singular surface in the medium and as expected, it is observed that the the amplitude of the jump in the velocity gradient satisfies the Bernoulli type transport equation. A particular case was considered to solve the transport equation numerically and to study the effects of dust particles and relaxation. The results are depicted and were found

**Table 1:** (a)–(c): Variations in amplitudes  $\alpha^{(3)}$  (transmitted waves),  $\beta^{(1)}$  (reflected waves) and  $|[\dot{V}]|$  (shock acceleration) in the influence of dust parameters  $k_p$ ,  $\beta$  and G in cylindrically symmetric flow.

		α <sup>(3)</sup>		β <sup>(1)</sup>		$ [\dot{V}] $	
		$lpha_0^{ ext{(1)}}>0$	$a_0^{(1)} < 0$	$a_0^{(1)} > 0$	$a_0^{\scriptscriptstyle (1)} < 0$	${\alpha_0^{\scriptscriptstyle (1)}>0}$	$\alpha_0^{(1)} < 0$
(a)							
$k_p$	0.2	0.00209196	-0.00099233	0.773758	-0.367039	-0.563106	0.267114
	0.4	0.00232379	-0.00108927	0.793081	-0.371757	-0.577673	0.270784
	0.6	0.00248798	-0.00118179	0.793908	-0.376489	-0.577791	0.274451
(b)							
β	0.1	0.00242578	-0.00113514	0.772793	-0.361627	-0.563347	0.263617
	0.5	0.00248798	-0.00118179	0.793908	-0.376489	-0.577791	0.274451
	1.0	0.00255018	-0.0011849	0.812423	-0.377479	-0.592236	0.275173
(c)							
G	100	0.00248798	-0.00118179	0.793908	-0.376489	-0.577791	0.274451
	1000	0.00205617	-0.00097668	0.793856	-0.377082	-0.57748	0.274303

to be consistent with the anticipation. As t approaches infinity for all the possible range of values of parameters involved in the flow such as  $k_p$ ,  $\beta$ , G, c, and  $\tau$ , the wave flattens and dies out eventually. It is observed that an increase in any of the parameters  $k_p$ ,  $\beta$ , or G leads an increase in  $\alpha^{(1)}$ . However, opposite behavior is noticed with an increase in the parameter  $\tau$ . It is also observed that an increase in any of the parameters  $k_p$ ,  $\beta$ , or G leads to an increase in  $\alpha^{(1)}/\alpha_0^{(1)}$  for the interval  $-\alpha_c^{(1)} \leqslant \alpha_0^{(1)} < 0$ , and a decrease in  $\alpha^{(1)}/\alpha_0^{(1)}$  for the interval  $\alpha_0^{(1)} \leqslant -\alpha_c^{(1)} < 0$ ; however, an increase in the variable  $\tau$  leads to an opposite trend.

**DE GRUYTER** 

The characteristic shock propagating in the medium is considered and it is observed that the values of jump in density and vibrational energy across the characteristic shock approach to zero as time tends to infinity. It is observed that with rise in the values of  $k_p$ ,  $\beta$ , or  $\tau$  leads to a rise in  $\zeta$ , whereas a rise in G leads to a fall in jump in density. Also, a rise in the values of  $k_p$ ,  $\beta$  or, G, gives a fall to the parameter  $\omega$  and a rise in  $\tau$  gives a rise to jump in vibrational energy.

The interaction between the singular surface and the characteristic shock is considered and it is observed that the amplitudes of the reflected wave, the transmitted wave and jump in the shock acceleration are directly proportional to the amplitude of the incident wave, i.e. a jump in the velocity gradient  $\alpha^{(1)}$ , thereby implying any increase or decrease in the incident wave will lead to an increase or decrease in the amplitudes of the reflected wave, the transmitted wave and jump in the shock acceleration. In the absence of the incident wave, there shall be neither a jump in the shock acceleration nor any reflected and transmitted waves. It is also observed that the amplitudes of the reflected wave, the transmitted wave and jump in the shock acceleration vary with the dust parameters separately from the incident wave. It is observed that depending on the incident wave being expansive (compressive), the reflected and transmitted waves are compressive (expansive), and the shock decelerates (accelerates) after the impact. The amplitudes of the reflected wave, the transmitted wave and jump in the shock acceleration increase with an increase in  $k_p$  or  $\beta$  in the case of  $\alpha_0^{(1)} > 0$  and decrease in the case of  $\alpha_0^{(1)} < 0$ ; however, an opposite trend is noticed in the case of an increase in *G*.

#### References

[1] M. Chadha and J. Jena, Comp. Appl. Math. 34, 729 (2014).

- [2] E. Varley and E. Cumberbatch, J. Inst. Math. Applics. 1, 101
- [3] A. C. Eringen and E. S Suhubi, Elastodynamics: Finite Motions, New York, Academic Press 1974.
- [4] P. J. Chen, Arch. Ration. Mech. Anal. 43, 350 (1971).
- [5] M. F. McCarthy, in: Continuum Physics (Ed. A. C. Eringen), 2, Academic Press, London 1975, p. 449.
- [6] A. Jeffrey, Appl. Anal. 3, 79 (1973).
- [7] A. Jeffrey, Quasilinear Hyperbolic Systems and Waves, Pitman, London 1976.
- [8] Ch. Radha, V. D. Sharma, and A. Jeffrey, Appl. Anal. 50, 145 (1993).
- [9] G. Boillat and T. Rugerri, Proc. R. Soc. Edin. 83A, 17 (1979).
- [10] G. Boillat and T. Ruggeri, Boll. Un. Mat. Ital. 15A, 197 (1978).
- [11] G. Boillat and T. Rugerri, Wave Motion 1, 149 (1979).
- [12] T. Ruggeri, Appl. Anal. 11, 103 (1980).
- [13] G. Boillat, C. M. Dafermos, P. D. Lax, and T. P. Liu, Lecture Notes in Mathematics on Recent Mathematical Methods in Nonlinear Wave Propagation, Springer, Berlin Heidelberg 1996.
- [14] A. Mentrelli, T. Ruggeri, M. Sugiyama and T. Zhao, Wave Motion 45, 498 (2008).
- [15] J. Jena, Math. Meth. Appl. Sci. 32, 2035 (2009).
- [16] Ch. Radha, V. D. Sharma, and A. Jeffrey, Appl. Anal. 50, 145 (1993).
- [17] A. Morro, Z. Angew. Math. Phys. 29, 822 (1978).
- [18] A. Morro, Acta Mech. 35, 197 (1980).
- [19] J. Jena, Theor. Comput. Fluid Dyn. 22, 145 (2008).
- [20] M. Pandey and V. D. Sharma, Wave Motion 44, 346 (2007).
- [21] J. Jena and R. Singh, Meccanica 48, 733 (2013).
- [22] J. Jena and R. Singh, Appl. Math. Comp. 225, 638 (2013).
- [23] J. Jena and V. D. Sharma, Int. J. Nonlinear Mech. 34, 313
- [24] M. Chadha and J. Jena, Int. J. Nonlinear Mech. 65, 164 (2014).
- [25] M. Chadha and J. Jena, Int. J. Nonlinear Mech. 74, 18 (2015).
- [26] M. Chadha and J. Jena, Meccanica **51**, 2145 (2016).
- [27] S. Shah and R. Singh, Phys. Fluids 31, 076103 (2019).
- [28] S. Shah and R. Singh, Int. J. Nonlinear Mech. 116, 173 (2019).
- [29] V. D. Sharma, Quasilinear Hyperbolic Systems, Compressible Flows and Waves, CRC Press, London (2010).
- [30] W. A. Scott and N. H. Johannesen, Proc. Roy. Soc. Lond. A 382, 103 (1982).
- [31] J. Jena and V. D. Sharma, J. Eng. Math. 60, 45 (2008).
- [32] J. K. Hunter, Asymptotic Equations for Nonlinear Hyperbolic Waves, in Surveys in Applied Mathematics, Vol. 2, (Eds. M. I. Freidlin, S. Gredeskul, J. Hunter, A. Marchenko, and L. Pasture), Springer Science+Business Media, New York 1995, p. 167.
- [33] S. I. Pai, Two Phase Flows, Vieweg Verlag, Braunschweig 1977.
- [34] G. Rudinger, Fundamentals of Gas Particle Flow, Elsevier Scientific Publishing Company, Amsterdam 1980.
- [35] H. Miura and I. I. Glass, Proc. R. Soc. Lond. 385A, 85 (1983).
- [36] M. Chadha and J. Jena, Comp. Appl. Math. 34, 729 (2015).
- [37] J. P. Vishwakarma and G. Nath, Meccanica 44, 239 (2009).
- [38] J. Hadamad, Lecons sur la propagation des ondes et les equations de l'hydrodynamique, Wentworth Press, Paris 1903.
- [39] T. Y. Thomas, J. Math. Mech. 6, 311 (1957).
- [40] T. Y. Thomas, Int. J. Eng. Sci. 4, 207 (1966).
- [41] D. Serre, System of Conservation Laws, 1, Cambridge University Press, New York 1999.
- [42] P. D. Lax, Commun. Pure Appl. Math. 10, 537 (1957).